ON THE INFLUENCE OF BEAM FILLING ON THE RESULTS OF MICROWAVE RETRIEVAL ALGORITHMS FOR CLOUD PARAMETERS

R.Bennartz [1] , M.Schaale, A.Thoss, P.Bauer [2] and J.Fischer
Institute for Space Sciences
Free University of Berlin, Germany

1 INTRODUCTION

A cloud and rain detection algorithm for the AMSU channels was derived using a new semi-statistical approach. Two datasets measured in March 1993 by the SSM/T2 and the SSM/I sensor onboard the DMSP F-11 satellite were taken as a basis for this examination. Only data located in the region of the North Sea and the Baltic Sea was taken into account (-10^o – 35^o E and 50^o – 75^o N). With these datasets classification algorithms of the Kohonen network type were performed for a combination of channels according to the future AMSU frequencies. Additionally, a set of radiative transfer calculations was carried out for all SSM/I and SSM/T2 channels. The clustering algorithm was applied to the model results, leading to relations between physical properties and the statistical results of the network and even presenting an opportunity to examine the accuracy of the clustering algorithm. Although no information about polarization differences was taken into account, a physically realistic classification algorithm was found.

2 METHODOLOGY

2.1 Clustering Algorithm

The Kohonen neural network can be placed in the class of unsupervised learning mechanism. It allows to describe even non-linear data distributions by a small set of representative points. The network is composed of n x m neurons (16 x 16 in this study) where every neuron is connected with its 4 nearest neighbours.

The learning algorithm takes two steps. In the first part, the neurons have to adapt their weights to the dataspace (in our case given as the x-dimensional space spanned by the brightness temperatures of the x choosen SSM/I and/or SSM/T2 channels). This process is controlled by two learning parameters denoted σ and ϵ, where σ is the half width value of a gaussian function located at every neuron and ϵ is the size of a learning step (for further details see Schaale and Furrer (1994)). As a result of the first step the neurons should represent the distribution of the data which was taken for training.

[1] Corresponding author address: Ralf Bennartz, Institute for Space Sciences, Free University of Berlin, Fabeckstr.69, 14195 Berlin, e-mail: bennartz@zedat.fu-berlin.de

[2] DLR, Cologne, Germany

In the second step the neurons have to be divided in distinct classes. This is done following an algorithm first published by Hillermaier et al.(1994). In this algorithm patterns on the network are induced (using the satellite data) and transformed treating the columns of a lateral connectivity matrix $\underline{C}$ as markov chains, where every matrix element C_{ij} stands for an activity hopping-probability from neuron j to neuron i. This leads to a linear spread out of the induced signal over the network. To come to stable patterns a non-linear acceleration term is applied increasing high activities and decreasing low activities. Using this mechanism every induced pattern will come to a stable state in a finite time. The number of different clusters depends on a paramter k which describes the ratio of the linear spreading to the non-linear acceleration (k can be compared with the temperature in simulated annealing cluster algorithms) and on a parameter A describing the activity zone around each neuron. For small values of k all input vectors are mapped to one cluster while for high values every neuron builds its own cluster. Plotting the number of distinct clusters against k in the transition range, the resulting function typically has a step structure where the length of each step is a measure of the stability of the clusters.

2.2 Radiative transfer model

All radiative transfer calculations were done using a polarized model based on the matrix operator theory (Bauer, 1992). Gaseous absorption was calculated using the algorithm of Liebe (1985). The emissivity of the ocean surface was parameterized according to Schluessel and Luthardt (1991). Different cloud types were adapted to the model with liquid water contents and droplet size distributions according to Silvermann and Sprangue (1970). All ice particles were assumed to be spherical and to have the same distribution as liquid water droplets. Both phases were allowed to occur at the same level, the relation between ice and liquid water was determined according to Wu and Weinman (1984). The droplet size distribution and intensity of rain was parameterized using the Marshall-Palmer approach. For size paramters greater than 0.1 Mie-scattering was applied.

The model was applied to 641 radiosoundings taken in the region of the North Sea over ocean in the period from April to September 1993. For 329 soundings a cloud free atmosphere was assumed. A cloudy atmosphere would have been choosen, if the relative humidity at one or more levels had exceeded 98 %, this was valid for 149 radiosoundings. In 163 cases rainy conditions were assumed.

3 RESULTS

3.1 Conventional statistical data analysis

The results of all types of clustering algorithms are strongly dependant on the input data and on the data preprocessing. To take this into account we first carried out some conventional statistical analysis (calculating correlation coefficients and principal component analysis (PCA)), which will be described briefly in the following subsection. One problem employing PCA is that channels having a broad range of brightness temperatures (e.g. the SSM/I channels at 19 GHz) contribute significantly more to the total variance and to the resulting principle components of the dataset than channels with small differences in brightness temperatures do (e.g. the SSM/T2 183/7 GHz channel). Therefore all brightness temperatures were scaled equal to a size from zero up to 255 adapting individual offsets and scales from histograms. This linear transformation does not affect the correlation coefficients, but overcomes the deficies of the PCA mentioned above.

To estimate the dimensionality of the classification problem correlation coefficients for all 12 channels were calculated (see Table 1). The correlation among the SSM/I channels is quite high. This is due to the great influence of the surface emissivity at frequencies lower the 100 GHz. Only the correlation coefficients for the channels at 19 GHz and 85 GHz are lower than 0.5. The influence of the water vapour absorption line at 22.235 GHz is very small, only the correlation coefficient among the 22 GHz channels and the 183-1 GHz channels is somewhat higher than the correlations among the 19 GHz or 37 GHz channels and the 183-1 GHz channel. For the SSM/T2 the 3 channels around the strong water vapour absorption line at 183.31 GHz can clearly be distinguished from the two window channels at 92 GHz and 150 GHz. Even the correlation coefficients among the three channels at 183 GHz are not higher than 0.8.

These results are also found employing principal component analysis. The first three eigenvalues are greater than one (See table 2), the fourth Eigenvektor explaines 3.4 % of the variance. With the first three components about 92.2 % of the total variance is achieved. The first eigenvector is mainly composed of the SSM/I channels and the SSM/T2 window channels while the frequencies around 183.31 GHz are contributing mainly to the second and third eigenvector.

This means that the maximum dimensionality of the dataspace for the combined SSM/I and SSM/T2 dataset is between five and six. From the SSM/I only two frequenies(one frequency lower than 50 GHz and one at 85 GHz) are representing independant information. For the SSM/T2 at least four channels contribute in a significant manner to the total variance of the dataset.

3.2 Clustering algoritms

For rain and cloud identification the channels at 183-1 GHz and 183-3 GHz are not of major interest because the maxima of there contribution functions (weighting functions) lie above 500 hPa or 700 hPa respectively and the water vapour accounts for 90 % of the attenuation even in situations with high liquid water clouds (Muller et al 1994).

To extract the channels which are mainly influenced by cloud liquid water, ice and rain the calculated brightness temperatures for the model calculations were plotted against the liquid water path, the ice path, rain rates, and the water vapour path. In figure 1 the 150 GHz brightness temperature is plotted against the temperature difference between the 150 GHz and 90 GHz channel. This channel combination is strongly influenced by changes in cloud liquid water content and rain rates. For fair weather conditions the temperature difference between the two window channels is not less than 20 K and increases with higher brightness temperatures (see figure 1. For cloudy conditions the temperature difference is smaller and the brightness temperature at 150 GHz is higher than it is for nice conditions. In rainy situations the temperature difference is almost less than 10 K and the brightness temperature is varying strongly. Although there are transition regions between cloudy and nice conditions and between rainy and cloudy conditions (due to light rain or thin clouds) three regions can be separated in the graph. The 183-7 GHz channel was examined in the same way, but the influence of water vapour was found to be too strong, so that it could not be taken into account. Thus, the 148 GHz channel and the difference between 148 GHz and 90 GHz were choosen as input for the clustering algorithm. Additionaly, the 22 GHz SSM/I channel was taken into account in order to separate footprints which are influenced by land surface. For AMSU applications this channel can easyly be replaced by the 23 GHz AMSU-A channel. About 15 % of the total dataset were randomly choosen for training. Figure 2 shows the classification graph, where the number of clusters is plotted against the learning paramter k (for the purpose of completeness the remaining learning parameters are also given). The length of each step in this graph is a measure of the stability of each cluster configuration. A very stable cluster configuration with 10 distinct clusters is found for k=1.5 up to k=2.0, this configuration is taken for further examinations.

Employing unsupervised learning mechanisms the crucial point is to allocate the found clusters to physical properties. In our case additional difficulties occur due to the missing in-situ data about rain rates and cloud liquid water contents. Therefore we applied the classification algorithm to the model data to join the clusters to the physical properties of the model atmospheres. This procedure yields a physical classification of the clusters as well as a statement about the correctness of the classification. In doing so two critical points have to be taken into account. First, the model results do not necessarily cover the whole range of measured brightness temperatures, and the model assumptions of e.g. cloud liquid water content, rain rates and scattering effects are not necessarily correct. This leads to the effect that some clusters will not be represented by the model results. Second, it is not possible to distinguish situations with low liquid water content or very light rain from cloud free situations, the signals do not differ adequately. Therefore classes with mixed information may occur, for which an exact classification can not be done. These problems are not founded on the clustering mechanisms, rather they are founded on the data itself and on the somewhat artificial partioning of a 45 km footprint into the three classes. As shown below, a cluster which is classified as 'nice or cloudy' can be associated with broken cloud fields.

The results of the classification are shows in table 3. A cluster was classified as rainy, cloudy or nice if more than 66 % of the points attached to the cluster were allocated to one of these classes. This yields to about 91 % correct classified model simulations. For rainy conditions about 19 % of the simulations were missclasified as cloudy or nice, for cloudy conditions 15 % were misclassified while for nice conditions only one simulations was misclassified. Keeping in mind the problems mentioned above, the clustering algorithm distinguishs the dataset in a suitable manner.

In figure 3 the classification algorithm was applied to the DMSP afternoon pass over the north sea for the 19th of March 1993 and the results compared to the corresponding Meteosat visible image (15:00 UTC) and a SSM/I cloud liquid water and rain retrieval algorithm (Bauer 1992) which was shown to work fairly well for the purpose of global retrievals. The southern edge of the cloudy region between England and Scandinavia is detected at 56^oN by the classification algorithm, this is in good accordance with the Meteosat image. The SSM/I retrieval algorithm detects clouds down to $54^o N$ where the Meteosat image does not show any clouds. At the area around $65^o N$ and $5^o W$ the classification detects a cloud free region although the Meteosat image shows a broken cloud field with partial very high grey values (i.e. high albedo). In the region north of about $65^o N$ the SSM/I algorithm detects only a few clouds, while the classification algorithm gives 'nice or cloudy' which seems more realistic.

The offshore rain areas around $60^o N$ are detected nearly in the same manner by both algorithms. Near to the coastlines both algorithms produce non-realistic rain fields. This is due to the varying surface emissivity which can falsify the signal in a strong way. Thus, including the 22 GHz channel did not yield the expected results.

4 SUMMARY AND CONCLUSIONS

A rain and cloud identification algorithm was derived using a new semi-statistical approach. In order to derive the channels with the most independant information, a classical statistical analysis including the calculating of principal components and correlation coefficients for all channels was employed. It was shown that for the purpose of classification 4 of the 5 SSM/T2 channels are giving independant information, while for the SSM/I sensor only 2 of the 7 channels are nearly uncorrelated. Analysing the results of a radiative transfere model, it was shown that from the future AMSU channels the window channels at 90 GHz and 150 GHz and the difference between those channels are giving the most information about cloudiness and rain. These channels were choosen as input for a new classification algorithm. The application of the algorithm to the model results gave a value of 91 % correct classified situations. For one DMSP pass the results of the algorithm were compared to results of a SSM/I cloud liquid water and rain retrieval algorithm and a corresponding Meteosat visible image. Although the classifications algorithm does not make use of polarization differences, it yields somewhat better results than the SSM/I algorithm (which was made for global applications).

For coastal regions several pixels were classified as rain, although the Meteosat image showed cloud free regions. In further investigations we hope to tackle this problem and to derive retrieval algorithms using a combination of visible, infrared and microwave data and including surface information using NDVI data.

5 ACKNOWLEDGEMENTS

The SSM/T2 data was assembled and provided by the Microwave Remote Sensing group of the Meteorology Department at Texas A&M University. The SSM/I data was distributed by National Snow and Ice Data Center at the University of Boulder, Colorado, USA.

6 LITERATURE

Bauer,P., 1992: Wasserdampf, Gesamtwasser und Niederschlagsrate aus Daten passiver Mikrowellenradiometer "uber dem Ozean. DLR-Forschungsbericht, DLR-FB 92-37.

Hillermaier, C. N.Kunstmann, B.Rabus and P.Travan, 1994: Topological feature maps with self-organized lateral connections: A population-coded one layer model of associative memory. Biol.Cybern. submitted and accepted.

Liebe, H.J. 1985: An updated model for millimeter wave propagation in moist air. Radio Science, 20, No.5, 1069-1089.

Muller, B.M., H.E. Fuelberg and X.Xiang, 1994: Simulations of the effects of water vapor, cloud liquid water, and ice on AMSU moisture channel brightness temperatures. J.Appl.Met., 33,1133-1154.

Schaale,M. and R.Furrer, 1994: Land surface classifications by neural networks. Int.J.Rem.Sens., submitted and accepted.

Schluessel, P. and H.Luthardt,1991: Surface wind speeds over ocean from Special Sensor Microwave/Imager observations. J.Geophys.Res.96, C3, 4845-4853.

Silverman, B.A. and E.D. Sprangue, 1970: Airborne measurements of in-cloud visibility. Nat.Conf. on Weather Modification of the AMS, April 6-9, Santa Barbara CA.

Wu, R. and J.A. Weinman, 1984: Microwave radiances from precipitating clouds containing aspherical ice, combined phase and liquid hydrometeors. J.Geophys.Res., 89, D5, 7170-7178.

GHZ	GHz 19v	GHz 19h	GHz 22v	GHz 37v	GHz 37h	GHz 85v	GHz 85h	GHz 92	GHz 150	GHz 183-1	GHz 183-3
19v	–	–	–	–	–	–	–	–	–	–	–
19h	+0.99	–	–	–	–	–	–	–	–	–	–
22v	+0.95	+0.95	–	–	–	–	–	–	–	–	–
37v	+0.94	+0.94	+0.94	–	–	–	–	–	–	–	–
37h	+0.92	+0.94	+0.92	+0.98	–	–	–	–	–	–	–
85v	0.47	0.48	+0.67	+0.66	+0.61	–	–	–	–	–	–
85h	+0.62	+0.66	+0.77	+0.79	+0.81	+0.90	–	–	–	–	–
92	+0.63	+0.66	+0.77	+0.72	+0.71	+0.79	+0.82	–	–	–	–
150	0.38	0.41	+0.60	0.50	0.48	+0.84	+0.78	+0.88	–	–	–
183-1	0.15	0.15	0.33	0.18	0.11	+0.56	0.36	0.48	+0.71	–	–
183-3	0.05	0.04	0.08	0.02	-0.04	0.18	0.01	0.16	0.25	+0.68	–
183-7	0.01	0.03	-0.06	-0.03	-0.05	-0.07	-0.12	0.09	-0.03	0.30	+0.82

Table 1 : Correlation coefficients between all SSM/I and SSM/T2 channels. Positive sign denotes correlation coefficients greater 0.5.

Eigenvector	1	2	3	4
Eigenvalue	7.19	2.40	1.48	0.48
Expl.Var.	59.9 %	20.0 %	12.3 %	3.4 %
19 GHz v	0.32	-0.17	0.32	-0.24
19 GHz h	0.33	-0.17	0.29	-0.20
22 GHz v	0.36	-0.09	0.13	-0.26
37 GHz v	0.35	-0.14	0.17	0.07
37 GHz h	0.34	-0.18	0.17	0.17
85 GHz v	0.31	0.14	-0.34	0.27
85 GHz h	0.33	-0.01	-0.24	0.41
92 GHz	0.33	0.10	-0.18	0.11
150 GHz	0.28	0.25	-0.39	-0.03
183-1 GHz	0.16	0.50	-0.17	-0.56
183-3 GHz	0.05	0.57	0.32	-0.05
183-7 GHz	-0.01	0.46	0.51	0.48

Table 2 : The first four eigenvectors for the combined SSM/I and SSM/T2 dataset with corresponding eigenvalues and achieved variances.

Cluster No.	Nice	Cloudy	Rainy	Classified as	Accuracy %
1	60	37	12	Nice or Cloudy	(89)
2	91	7	0	Nice	93
3	104	17	3	Nice	84
4	0	24	11	Cloudy	69
5	0	7	5	Cloudy or Rainy	(100)
6	50	5	0	Nice	91
7	0	48	59	Cloudy or Rainy	(100)
8	0	0	16	Rainy	100
9	23	2	8	Nice	70
10	1	2	49	Rainy	93
Total	329	149	163		

Table 3 : Results of the application of the clustering algorithm to the model brightness temperatures. The clusters were classified according to the criterion that more than 66 % of the points allocated to one cluster belong to one physical situation.

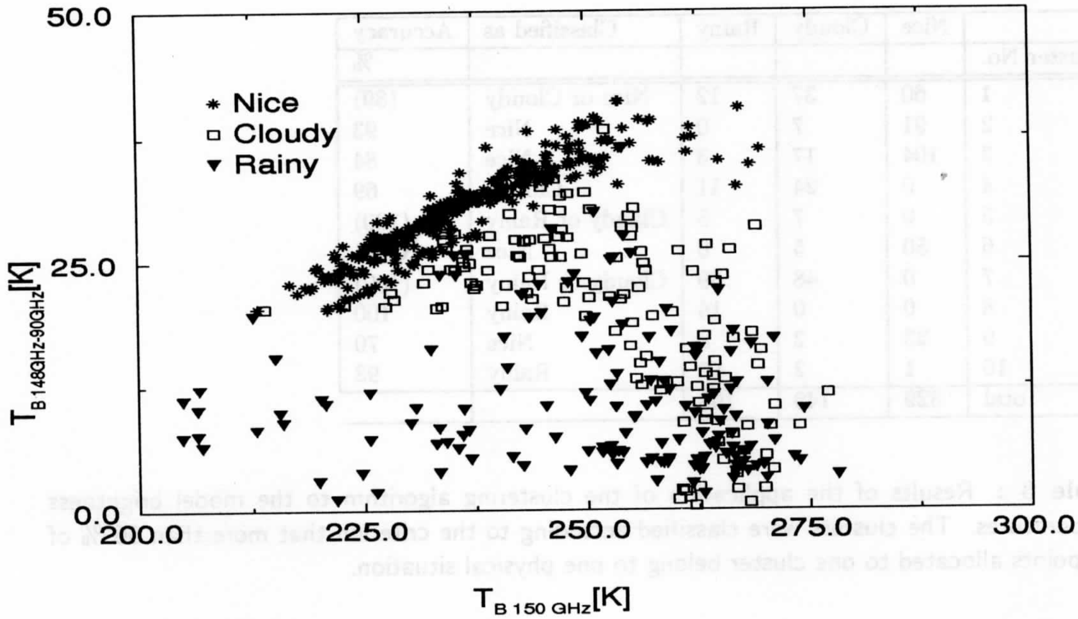

Figure 1 : Brightness temperature difference between the 150 GHz and the 92 GHz channel against the brightness temperature at 150 GHz for all model runs.

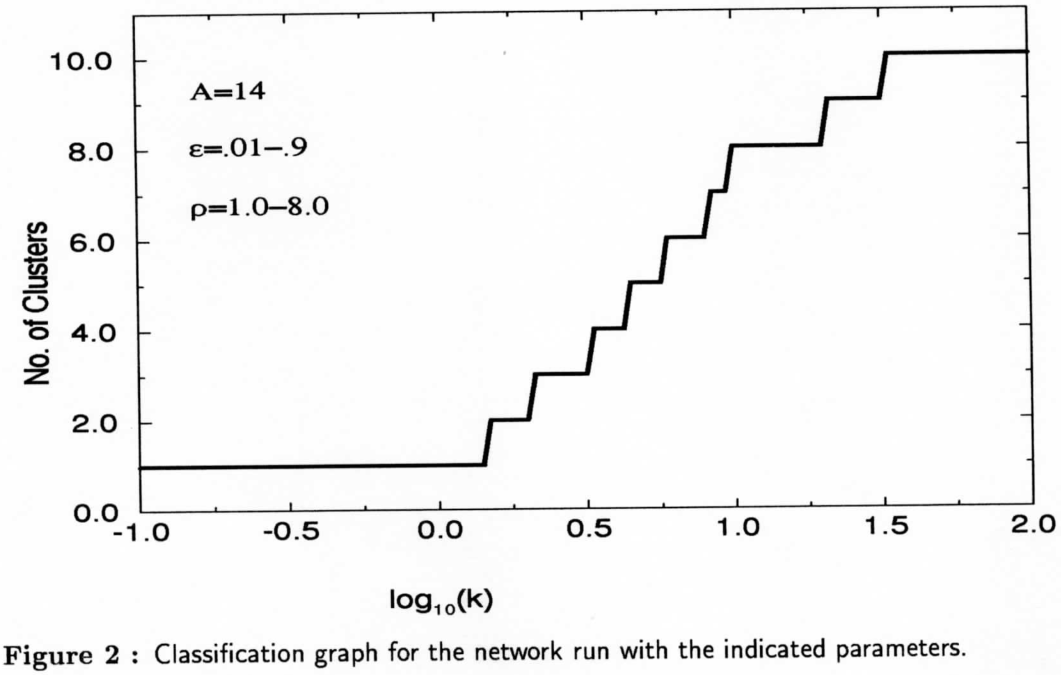

Figure 2 : Classification graph for the network run with the indicated parameters.

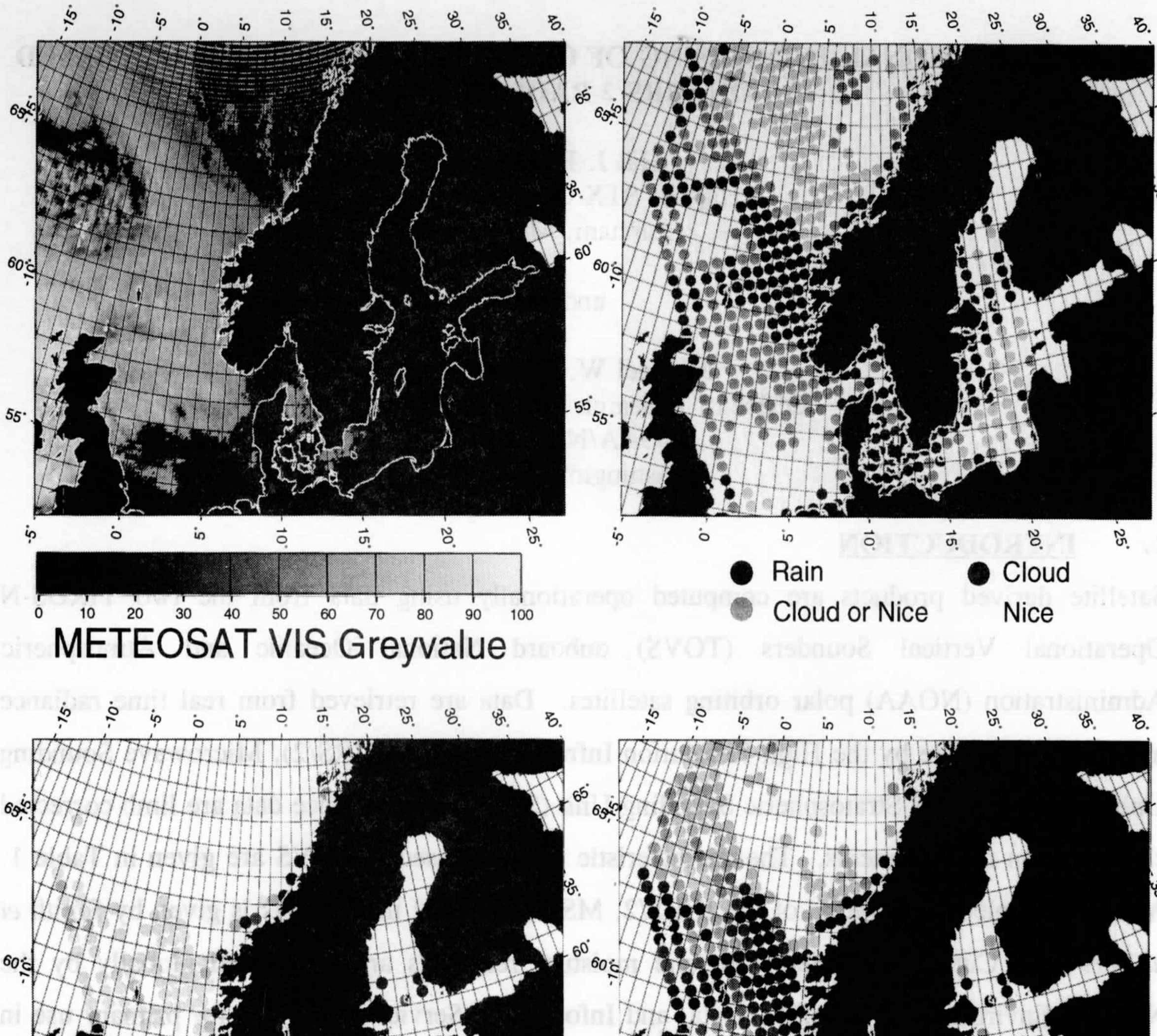

Figure 1 : Intercomparison between the classification algorithm, a SSM/I cloud and rain retrieval algorithm and the corresponding Meteosat visible image for 19th March 1993 15:00.

TECHNICAL PROCEEDINGS OF

THE EIGHTH INTERNATIONAL TOVS STUDY CONFERENCE

Queenstown, New Zealand

5-11 April 1995

Edited by

J R Eyre

Meteorological Office, Bracknell, U.K.

Published by

European Centre for Medium-range Weather Forecasts
Shinfield Park, Reading, RG2 9AX, U.K.

July 1995